History of Medicine Studies

ISSN:1300-669
Volume 13 Issue 2 July 2017

Femtosecond Laser Scribing of $Cu(In,Ga)Se_2$ Thin-Film Solar Cell

Aiko Narazakai, Ryozo Kurosakii, Tadatakiie Satoo,

The photovoltaic properties of two types of electrically isolated laboratory-scale Cu(In,Ga)Se2 (CIGS) solar cells were compared: "Type 1" with complete removal of both the transparent conductive oxide (TCO) and CIGS layers, and "Type 2" with complete removal of only the TCO layers. As the shunt resistance dropped dramatically with "Type 1" scribing, the photovoltaic efficiency dropped along with it. The shunt resistance did not suddenly reduce after the "Type 2" scribing, hence the overall efficiency was not drastically affected. For "Type 2" scribing, the efficiency reduction was just 0.1 percentage points, but for "Type 1" it was often 1.3 percentage points. An electron-beam-induced current (EBIC) investigation was also carried out to look into the impact of laser irradiation on a buried p-n junction in the "Type 2" laser-scribed CIGS solar cells. Thus, EBIC signals were clearly seen along a sidewall of the laser-scribed trench, demonstrating that the p-n junction was preserved even after our femtosecond laser scribing. For CIGS solar cells, femtosecond laser scribing is a useful technique that maintains high efficiency.

Keywords: Photovoltaic efficiency, shunt resistance, femtosecond laser scribing, CIGS solar cells, and EBIC cells

1. Introduction

One of the most promising thin-film solar cells is chalcopyrite Cu(In,Ga)Se2 (CIGS) due to its high efficiency, which may reach > 20% for the laboratory-scale single cells [1,2]. ZSW [1] has just attained the greatest efficiency of 21.7%. Due to its great resistance for exposure to sunlight, CIGS thin-film solar cells have also gained consideration for use in space applications [3]. greater photocurrent and the resulting resistance loss in a TCO layer tend to reduce the efficiency of thin-film solar cells with a greater active area. For this reason, solar cells with a high surface area are often separated into many smaller pieces and linked in series to minimize resistance loss. Three scribing processes, designated P1, P2, and P3, are responsible for the linking. To isolate individual circuit elements, the P1 scribes a back contact layer adjacent to the substrate. The P2 is required for the series connectivity by electrically linking the back and front contact layers of neighboring cells. Finally, the electrical isolation between neighboring cells is created by the P3 scribe in the front contact layer. reports of CIGS scribing have been made [4-11]. Using a range of laser sources and pulse durations (from 0.1 to 250 ns), Compaan et al. [4] demonstrated laser ablation of polycrystalline films, including CIGS. They investigated how laser factors including pulse duration, wavelength, and fluence affected the form of the trench. They discovered that a longer nanosecond pulse was optimal for selectively removing the CIGS layer from the molybdenum (Mo) back contact layer. However, irradiating CIGS with a nanosecond pulse laser resulted in excessive melt formation and/or the precipitation of less refractory phases owing to laser-induced heat production [5]. This novel approach for replacing the mechanical P2 utilizes a CIGS structure that has been laser-modified to reduce resistance. A drop in shunt resistance and efficiency might result from the emergence of lesser resistive phases in the P3. Ultrashort-pulse lasers are preferable for eliminating the CIGS layer because of a process known as cold ablation, which reduces the thermal impact of the process [6-11]. Melt formation on a sidewall of CIGS in the P3 trench nonetheless tended to emerge despite the successful reduction of a heat-affected zone (HAZ), lowering the efficiency of the solar module. A novel P3 scribing was investigated to see whether it may help boost productivity any more. Lift-off generated by laser ablation of a CIGS layer's top surface destroyed just the top TCO contact layer entirely [10].

*1 *Research Institute for Sustainable Chemistry, National Institute of Advanced Industrial Science and Technology (AIST), Central 5, 1-1-1 Higashi, Tsukuba, Ibaraki 305-8565, Japan*
E-mail: Aiko Narazakai @aist.go.jp

History of Medicine Studies
ISSN:1300-669
Volume 13 Issue 2 July 2017

In this work, we have made a comparative study of photovoltaic properties of laboratory-scale Cu(In,Ga)Se_2 (CIGS) solar cells electrically-isolated from each other by two types of femtosecond laser scribes: “Type 1” with removing both transparent conductive oxide (TCO) and CIGS layers and “Type 2” with complete removal of only TCO. Both of scribes correspond to the P3 in module fabrication. Further, in order to investigate the laser irradiation effect on a buried p-n junction in the CIGS solar cell, an electron-beam-induced current (EBIC) analysis was performed.

2. Experimental

Film deposition for CIGS solar cell

For CIGS solar cell fabrication, film deposition was performed by our AIST team on a 30 × 30 mm soda lime glass substrate. The layered structure was, from the bottom to the top, a sputtered 1-μm thick Mo back contact, a co-evaporated 2-μm thick CIGS absorber [12], a chemical bath depositing 60-nm thick CdS buffer, a sputtered 60-nm thick i-ZnO buffer, a sputtered 350-nm thick Al-doped ZnO (n-ZnO used as TCO), and Al grids, as shown in the first step in Fig. 1 (a).

Scribing and *J-V* evaluation of small-area CIGS solar cells

Thus-obtained sample was divided into 8 small-area cells by mechanical scribing with removing TCO and CIGS layers completely, as shown at the second step in Fig. 1 (a). The mechanical scribing was denoted by blue line in Fig. 1 (b). The individual small-area CIGS solar cell surrounded by the blue line has an active area of approximately 0.5 cm^2. In order to study the change of laser scribing on the photovoltaic efficiency before and after laser scribing in detail, the efficiency was evaluated at first for the CIGS single solar cell isolated by only the mechanical scribing. Current density-voltage (*J-V*) measurements were performed under standard conditions: 298 K, 100 mW· cm^{-2}, AM 1.5 G in-house. The shunt resistance was measured in a dark condition. These efficiency and shunt resistance were used as initial values before laser scribing. At the fourth stage of Fig. 1 (a), femtosecond laser scribing was applied to the CIGS single cell as denoted by red line in Fig. 1 (b). The scribe length was about 5 mm. We tested two types of laser scribing: “Type 1” of complete removal of both TCO and CIGS layers and “Type 2” of complete removal of only TCO. Both of scribes made the electrical isolation in the TCO between adjacent cells, corresponding to the P3 scribe in module preparation. Hereafter, we call these scribes “Type 1” and “Type 2” P3. Finally, the *J-V* measurements were carried out for the laser-scribed cells. Here, it should be mentioned that the cell active area was corrected after laser scribing to calculate the efficiency and shunt resistance accurately.

Laser scribing system

Figure 2(a) shows schematic of a femtosecond laser (300 fs, 100 kHz) used for the laser scribing in this work, which was developed by our AIST team. Via the second-

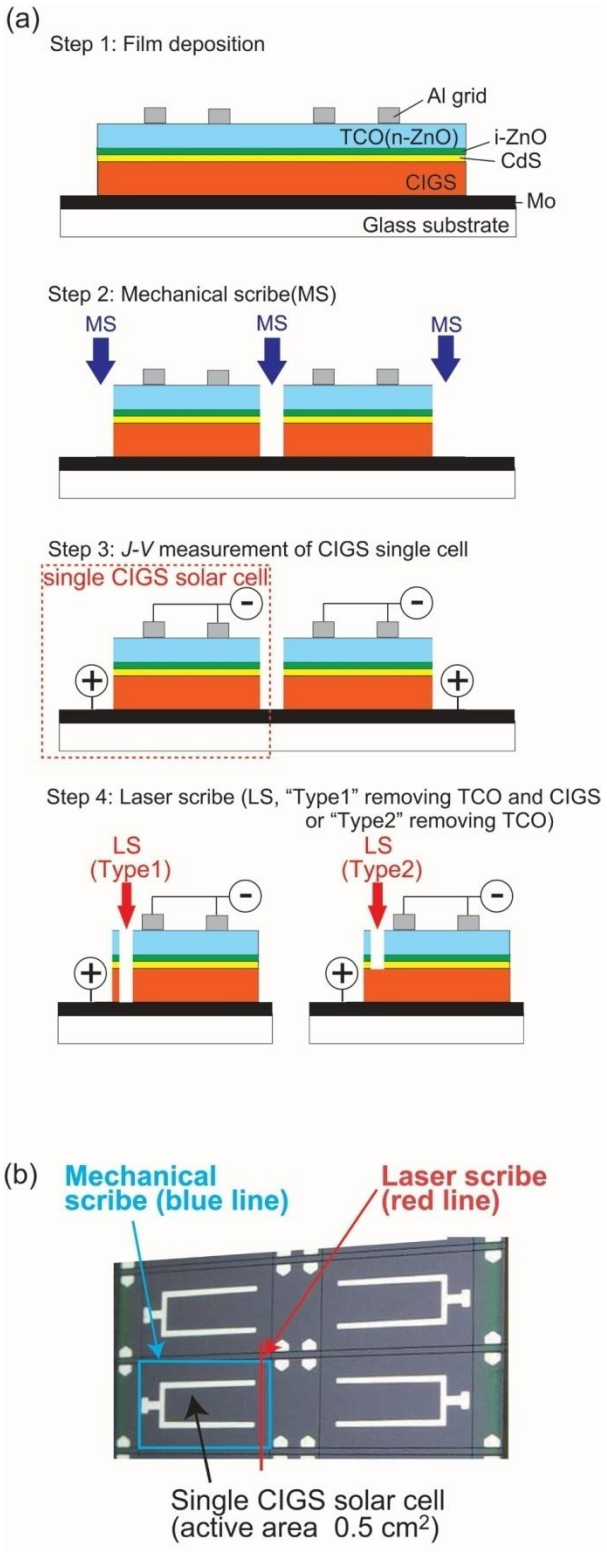

Fig. 1 (a) Schematic diagrams of our evaluation steps of laser-scribed CIGS single solar cell. (b) Top-view photograph of four CIGS single solar cells. First, single cells were separated from each other by mechanical scribe (blue line). The photovoltaic efficiency was measured as an initial value. Secondly, laser scribing (red line) was performed. Finally, the efficiency of the laser-scribed cell was evaluated.

History of Medicine Studies
ISSN:1300-669
Volume 13 Issue 2 July 2017

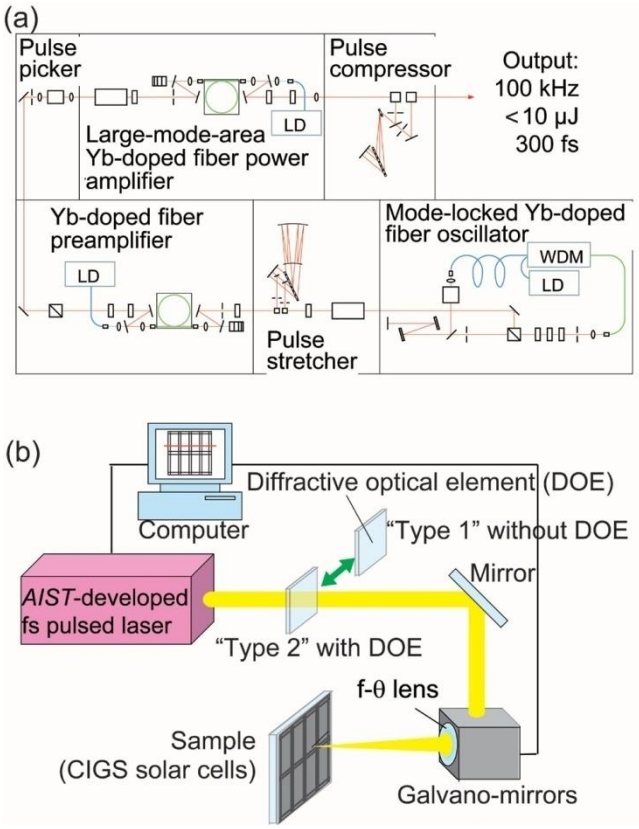

Fig. 2 (a) Schematic of our femtosecond (fs) pulsed laser with Yb-doped fiber chirped-pulse amplification system. (b) Setup for laser scribing of CIGS solar cells using the AIST-developed fs pulsed laser in Fig. 2(a) and galvano-mirrors / f-θ lens system. Diffractive optical element (DOE) was inserted to change the beam profile in the case of "Type 2" scribing.

harmonic generation, the laser pulse with a central wavelength of 517 nm was irradiated onto the CIGS sample under atmospheric and room-temperature condition.

The laser pulse was focused onto a top surface of the sample through a telecentric f-θ lens, as shown in Fig. 2(b). The laser spot was scanned by using galvano-mirrors at a scan rate of 1 m· s^{-1}. The original laser beam had a circular Gaussian profile. For the "Type 1" scribe, the original laser beam was used. The circular focal spot has a diameter of about 25 μm. Thus, the beam overlapping rate was 60 %.

On the other hands, for the "Type 2" scribing, we used a square-shaped laser beam with a nearly-top-hat profile. Because scribing thin films with circular Gaussian beam generally causes formation of non-smooth edges and damage or excess modification in overlapping areas, a flat-top square-shaped beam is ideal for laser scribing [11]. Diffractive optical element (DOE) was used for beam-shaping the original circular Gaussian beam into a nearly-top-hat beam with a square shape of about 20 × 20 μm at the focal point. The beam overlapping rate was 50 %. The energy loss caused by the DOE was approximately 5 % of the incident laser energy. Hereafter, the laser pulse energy and fluence denote the energy after the f-θ lens and fluence at a sample surface, respectively.

For the "Type 2", the scribe was done twice to remove a TCO layer completely. In most cases, the TCO can be removed by a single scan. However, with decreasing the laser fluence to diminish laser-induced damage, incomplete removal of TCO sometimes occurred. Thus, in order to achieve complete "Type 2" scribe, two-pass scribing was conducted in this work.

For the "Type 1", it was difficult to etch the CIGS layer completely with the beam-shaped pulse under 10 pass. Thus, we concentrated on scribing without DOE in the case of "Type 1" in this work.

Morphology and EBIC observation

The surface morphology of the laser-scribed trenches was examined with a confocal laser scanning microscope (Keyence VK-8500) and a high-resolution field emission scanning electron microscope (FESEM; HITACHI S4800). In order to investigate the effect of laser scribing on a buried p-n junction of CIGS solar cells, electron-beam-induced current (EBIC) measurements in the FESEM were also carried out [13].

3. Results and discussion

Morphology of laser-scribed trench

Figure 3 (a) shows the dependence of trench depth etched by scanning of the circular Gaussian beam on the pass number of laser scribe. The laser pulse energy was 3.5 μJ after the f-θ lens, which is a maximum of our laser scribing system. The laser fluence at the sample surface was about 0.71 J· cm^{-2}. After the first pass, the TCO(n-ZnO)/i-ZnO/CdS layers were eliminated. Since typical band gap is 3.37 eV for ZnO and 2.42 eV for CdS, these materials are nearly transparent for the single photon absorption. Thus, the laser pulse through these layers might be strongly absorbed at a top of CIGS absorber layer, resulting in complete removal of the TCO/i-ZnO/CdS by a lift-off process caused by the laser ablation of a top of CIGS. In some cases of ultrashort laser pulse-material interaction, the nonlinear absorption leads to the ablation of transparent materials without linear absorption. However, the lift-off process of TCO/i-ZnO/CdS layers caused by ablation of CIGS layer was observed to be dominant in the laser fluence range employed in this work. Thus, the contribution of nonlinear process might be small.

With increasing the number of scribes, the laser ablation of CIGS proceeded. After the forth pass, a surface of Mo back contact appeared at a center of the trench bottom, which corresponds to the "Type 1" scribe.

Figure 3 (b) demonstrates confocal laser scanning microscopic image and cross-sectional profile of the "Type 1" trench produced by 4 times scribes under the same condition with Fig. 3 (a). Due to the Gaussian beam profile, the trench has a taper shape. Whereas the TCO layer was removed with a width of about 25 μm, the Mo surface appeared at the trench bottom with only about 5-μm width. It was observed that the smooth surface of CIGS was left on a trench sidewall, suggesting that the CIGS layer formed a melt pool by the laser irradiation followed by the resolidification. The CIGS melt formation might be caused

History of Medicine Studies
ISSN:1300-669
Volume 13 Issue 2 July 2017

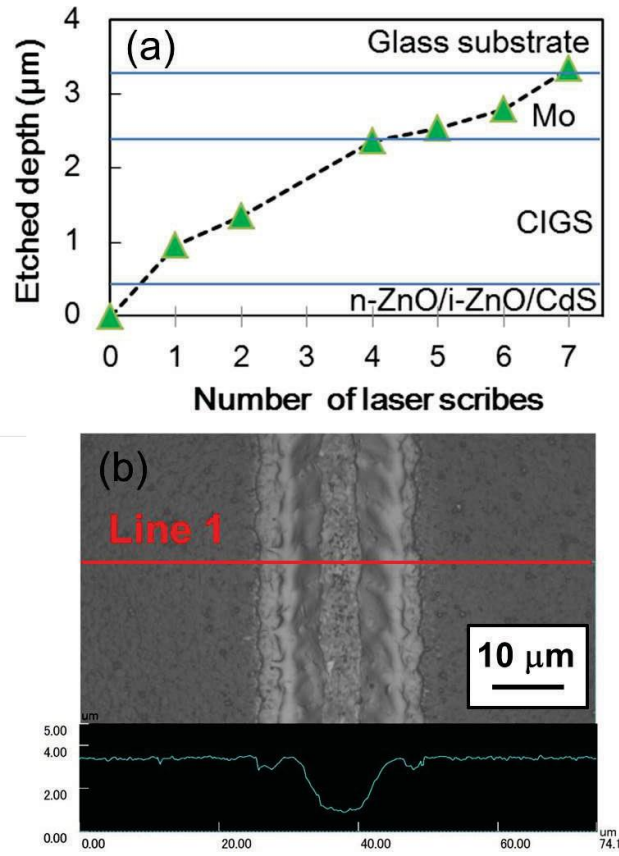

Fig. 3 (a) Dependence of the etched depth at a laser beam center on the number of laser scribes. The laser fluence at the sample surface was about 0.71 J· cm^{-2}. (b) Confocal laser scanning microscopic image and cross-sectional profile at Line 1 of a trench laser-scribed 4 times under the same condition with (a). Both the n-ZnO and CIGS layers were removed completely at the beam center, which corresponds to the "Type 1" scribe.

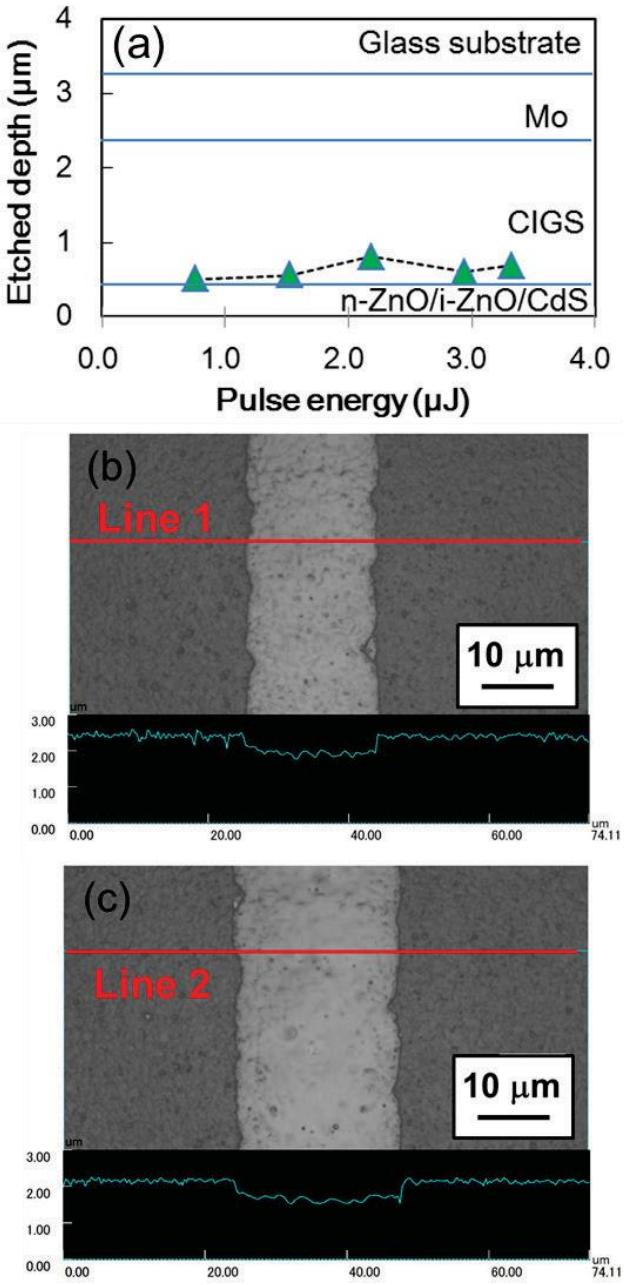

Fig. 4 (a) Dependence of the etched depth on the laser pulse energy. The nearly-top-hat beam with a square shape through DOE was irradiated. The laser pulse energy at the sample surface varied from 0.8 to 3.3 μJ, corresponding to the laser fluence from 0.2 to 0.83 J· cm^{-2}. Confocal laser scanning microscopic images and cross-sectional profiles of the trenches scribed at (b) 0.8 and (c) 2.2 μJ, respectively. The TCO/i-ZnO/CdS layers were completely removed, which corresponds to "Type 2" scribe.

by the single-pulse and/or multi-pulse laser irradiation, although it is not clear whether which played a main role in this work.

Different from the "Type 1" scribe, "Type 2" scribe needs to eliminate only TCO. Hence, the laser beam was scanned only twice to remove TCO absolutely in this work. Furthermore, since the main purpose of "Type 2" scribe was to diminish the CIGS melt, we tested laser scribing at lower laser pulse energy to do damage control.

Figure 4 (a) shows the dependence of etched depth on laser pulse energy. Through an entire laser pulse energy employed in this work from 0.8 to 3.3 μJ, the etched depth increased from 500 to 700 nm. The corresponding laser fluence was 0.2 to 0.83 J· cm^{-2}. Since the TCO layer was eliminated completely, the "Type 2" scribe was achieved. Although the laser pulse energy became about 4 times, the etched depth increased only 1.4 times. This fact also indicates that the etching mechanism is based on the lift-off of TCO with a thinness of 350 nm initiated by the laser ablation of a top of CIGS layer.

Confocal laser scanning microscopic images of the "Type 2" trenches scribed at 0.8 and 2.2 μJ are shown in Figs. 4 (b) and (c), respectively. The trench width increased from 19 μm at 0.8 μJ to 24 μm at 2.2 μJ. The increase in the width stems from shoulders of nearly top-hat profile beam-shaped by the DOE. In addition, the trench bottom etched at 2.2 μJ was smoother than that etched at 0.8 μJ,

History of Medicine Studies
ISSN:1300-669
Volume 13 Issue 2 July 2017

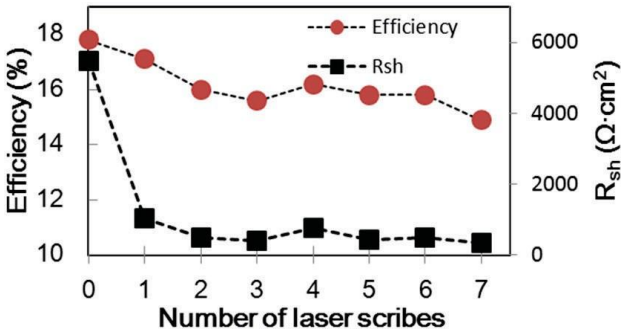

Fig. 5 Variation of photovoltaic properties with number of laser scribes. The scribing condition was same with that in Fig. 3. The laser fluence at the sample surface was about 0.71 J· cm^{-2}. The red circles and black squares denote the efficiency and shunt resistance, respectively.

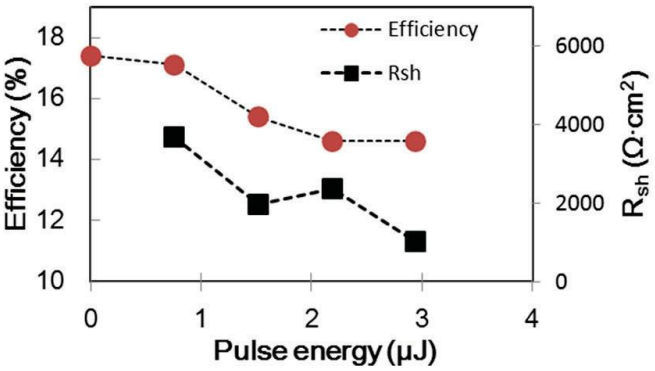

Fig. 6 Variation of efficiency and shunt resistance with pulse energy for "Type 2" laser scribing. The laser irradiation condition was same with that in Fig. 4.

suggesting the laser-induced formation of melt pool at higher laser pulse energy.

3.2 Changes in photovoltaic properties after laser scribing

As reported in previous studies by other groups, photovoltaic properties such as the shunt resistance and efficiency of CIGS solar cells decreased even after ultrashort laser scribing [7,8]. In order to explore the effect of laser scribing on photovoltaic properties in detail, we evaluated the properties before and after laser scribing in this work.

Figure 5 plots solar cell efficiency (red circles) and shunt resistance R_{sh} (black squares) versus the number of laser scribe under the same condition with Fig. 3 (a). The shunt resistance drastically dropped from over 5.5 × 10^3 Ω·cm^2 to below 1.0 × 10^3 Ω·cm^2 after the first scribe. With an increase in the scribe number, the shunt resistance further decreased. For solar cells, a decrease in the shunt resistance is undesirable because it often leads to decrease solar cell efficiency. To keep a high shunt resistance, it is vital to suppress the shunt formation within the solar cell during P3 scribe. In the case of CIGS solar cells, the laser irradiation below its ablation threshold easily produced melt formation followed by the precipitation of lower-resistant phases such as Cu-rich phase and Cu_xSe [5,6]. Based on the laser microscopic image shown in Fig. 3 (b), the CIGS layer at the trench sidewall experienced the excess melt and re-solidification caused by the laser irradiation, leading to a decrease in the drastic shunt resistance. The solar cell efficiency also decreased after laser scribing. For the "Type 1" trench made by 4 times scribes shown in Fig. 3 (b), the R_{sh} and the efficiency were 7.6 × 10^2 Ω·cm^2 and 16.2 %, respectively. Typical drop of the efficiency was 1.3 for the "Type 1" scribe. The cell scribed by a single pass exhibited higher efficiency compared to that scribed by four passes. Thus, the depth of the laser-scribed trench affected the cell performance under the same beam profile condition.

Figure 6 shows solar cell efficiency (red circles) and shunt resistance R_{sh} (black squares) versus the laser pulse energy for the "Type 2" scribe. The scribe condition was same with that of Fig. 4 (a). Different from the drastic decrease in the shunt resistance for the "Type 1" as shown in Fig. 5, the shunt resistance was 3.7 × 10^3 Ω·cm^2 at the lowest pulse energy of 0.8 μJ. With increasing the pulse energy, the shunt resistance decreased and finally dropped to 1.0 × 10^3 Ω·cm^2 at 2.9 μJ. As shown in Fig. 4 (a), when the pulse energy increased from 0.8 to 2.2 μJ, the etched depth increased from 500 to 700 nm and the surface morphology of the trench bottom became smoother. This indicates that the melt of CIGS layer occurred in the case of "Type 2" scribe at higher pulse energy as well as the "Type 1" case. As a result, 0.8 μJ is suitable for preventing from a drop in the shunt resistance. At optimum pulse energy of 0.8 μJ, the solar cell efficiency of 17.1 % was achieved. The drop in the efficiency was suppressed to 0.1 from the original value of the mechanical-scribed cell. At higher pulse energy, the efficiency became lower. The decrease in the shunt resistance and resultant solar cell efficiency might be caused by the laser-induced structure of CIGS with lower resistance. Thus, for laser scribing of "Type 2" as well as "Type 1", it is desirable to avoid the unnecessary laser irradiation onto CIGS layer.

3.3 EBIC observation and *J-V* curve of "Type 2"-scribed trench

Finally, "Type 2" trench fabricated at the optimum condition in Fig. 6 was characterized by EBIC measurements in order to investigate the femtosecond laser irradiation effect on a buried p-n junction. Although the EBIC is not suitable for testing across large-area samples, EBIC can reveal the cell character like the p-n junction and microstructures concurrently. For example, lock-in thermography (LIT) is a valuable tool for testing large-area solar cells. Johnston et al. identified defects with a size of several micrometers as shunt and weak diode by a combination of LIT and SEM [14]. However, LIT measurements have too poor spatial resolution to observe small defects, which first appeared as a problem for relatively-uniform and high-

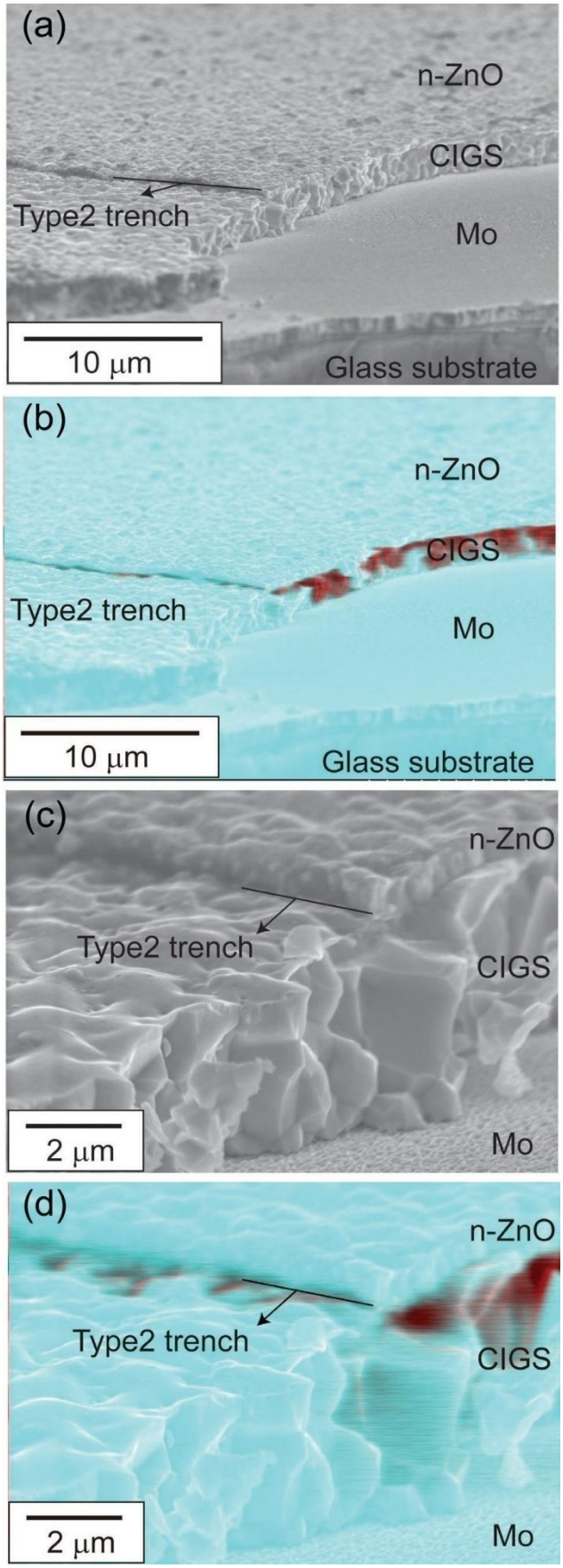

Fig. 7 (a,c) SEM and (b,d) EBIC cross-sectional images of "Type 2"-scribed trench. Figures (c) and (d) are magnified images. The red-colored area in the EBIC images indicates a photo-generated region.

efficient solar cells [8]. In this work, we introduced EBIC measurements in order to investigate the effect of laser irradiation on a buried p-n junction, which is important for the cell performance, for high-efficient solar cells.

Figure 7 (a) shows a SEM nearly-cross-sectional image of the "Type 2" trench. After complete removal of n-ZnO (TCO) by laser scribing, a sample was prepared by cleaving cross the trench. Figure 7 (b) shows an EBIC image corresponding to the SEM image of Fig.7 (a). The red-colored area of the EBIC image indicates a photo-generated region, that is a space-charge region (SCR) plus the minority carrier diffusion length. The SCR (red-colored parts) was clearly observed along the trench, indicating the existence of p-n junction just around the trench sidewall. Magnified SEM and EBIC images are also shown in Figs. 7 (c) and (d), respectively. Based on the magnified SEM image, a CIGS surface at a trench bottom is smoother than an as-prepared CIGS surface, due to laser-induced melt experience. This smooth layer is very thin with a thickness less than 100 nm from this SEM resolution. In Fig. 7 (d), EBIC signals were clearly observed from the cleaved CIGS layer as well as the trench sidewall. Particularly, the intense EBIC signal was observable from an upper part of the cleaved CIGS layer just around the trench. This is because a p-n junction of CIGS solar cells generally exists in an upper part of CIGS layer. The Cd diffusion from a CdS buffer layer into a p-type CIGS layer forms a p-n junction in the upper part of the CIGS layer [13]. The resolution of our EBIC measurement was submicron. Therefore, the p-n junction still survived even in the region adjacent to the "Type 2" trench.

In the case of "Type 1" scribe, HAZ was formed mainly around trench sidewalls in CIGS layer, as shown in Fig.3: the sidewalls obviously experienced the excess melt formation followed by re-solidification. Although HAZ might be formed at both sidewalls and bottom of the trench in the case of "Type 2", there seemed less damage like melt formation compared to "Type 1" due to lower laser fluence necessary for the process. In fact, EBIC results in Fig. 7 clearly show the working p-n junction just around the sidewalls, suggesting similar situation at the trench bottom. Consequently, "Type 2" femtosecond laser scribing is an effective tool for high-speed and small-dead-area cutting with keeping high efficiency.

4. Summary

A comparative study of photovoltaic properties of laboratory-scale CIGS solar cells electrically-isolated from each other by two types of femtosecond laser scribes was performed: "Type 1" with removing both TCO and CIGS layers and "Type 2" with complete removal of only TCO. The shunt resistance drastically decreased in the case of the "Type 1" scribing, degrading the photovoltaic efficiency. The "Type 2" scribing did not accompany a sharp drop in the shunt resistance, keeping relatively-high efficiency. The difference in the efficiency between before and after the "Type 2" scribing was only 0.1, while a typical drop for the "Type 1" was 1.3. Based on EBIC measurements for "Type 2"-scribed cell, EBIC signals were clearly observed along a sidewall of the laser-scribed trench, indicating that the p-n

ISSN:1300-669
Volume 13 Issue 2 July 2017

junction survived after our femtosecond laser scribing even at the sidewall of the laser-scribed trench. Ultrashort-pulsed laser scribe with complete removal of TCO is a promising technology for CIGS solar cells with high efficiency.

References

[1] ZSW press release (22 September 2014) [http://www.zsw-bw.de/uploads/media/pr12-2014-ZSW-WorldrecordCIGS.pdf]
[2] Solar Frontier HP [http://www.solar-frontier.com/eng/news/2014/C031367.html]
[3] S. Kawakita, M. Imaizumi, M. Yamaguchi, K. Kushiya, T. Ohshima, H. Ito and S. Matsuda: Proc. 2nd World Conf. Photovoltaic Energy Conversion, Vienna, (1998) 3568.
[4] A. D. Compaan, I. Matulionis and S. Nakade: Opt. Lasers Eng., 34, (2000) 15.
[5] P-O. Westin and M. Edoff: 23rd European Photovoltaic Solar Energy Conference, Valencia, (2008) 2558.
[6] D. Ruthe, K. Zimmer and T. Höche: Appl. Surf. Sci., 247, (2005) 447.
[7] A. Wehrmann, H. Schulte-Huxel, M. Ehrhardt, D. Ruthe, K. Zimmer, A. Braun and S. Ragnow: Proc. of SPIE, 7921, (2011) 79210T.
[8] P. Gecys, G. Raciukaitis, A. Wehrmann, K. Zimmer, A. Braun and S. Ragnow: Journal of Laser Micro/Nanoengineering, 7, (2012) 33.
[9] A. Burn, M. Muralt, R. Witte, S. Buecheler, S. Nishiwaki, L. Krainer, G. J. Spuehler and V. Romano: Proc. of SPIE, 8967, (2014) 896717.
[10] E. Markauskas, P. Gečys and G. Račiukaitis: Proc. Of SPIE, 9350, (2015) 93500S-1.
[11] G. Račiukaitis, E. Stankevičius, M. Gedvilas, C. Bischoff, E. Jäger, U. Umhofer and F. Vöolklein: Journal of Laser Micro/Nanoengineering, 6, (2011) 37.
[12] Y. Kamikawa-Shimizu, H. Komaki, A. Yamada, S. Ishizuka, M. Iioka, H. Higuchi, M. Takano, K. Matsubara, H. Shibata and S. Niki: Applied Physics Express, 6 , (2013) 112303.
[13] S. Kijima and T. Nakada: Appl. Phys. Express, 1, (2008) 075002.
[14] S. Johnston, T. Unold, I. Repins, R. Sundaramoorthy, K. M. Jones, B. To, N. Call and R. Ahrenkiel: J. Vac. Sci. Technol. A, 28, (2010) 665.

(Received: June 11, 2015, Accepted: February 4, 2016)